

# Hydrologic Investigations in the North Chilean Altiplano Using Landsat - MSS and - TM Data

Mathias Vuille & Michael F. Baumgartner

Institute of Geography  
University of Berne  
Hallerstr. 12  
3012 Berne, Switzerland

## Abstract

*In order to understand Late Glacial high lake levels in the dry Andes of Northern Chile, recent short - to medium-term fluctuations in the water budget of present lakes and brines (salars) and their relationship with the atmospheric circulation were investigated. A time sequence of four Landsat-MSS images between November 1983 and August 1984 was analysed in terms of changing water surface and water volume of several lakes and salars. The variations of the open water bodies were interpreted as a result of the spatial pattern of summer and winter precipitation. Furthermore a method to determine water depth and water salinity of the very shallow salars and lakes by correlating field measurements and digital Landsat-TM data is described. The resulting model to compute water depth was also applied to the MSS-sequence, showing good results.*

## Introduction

The extremely dry Atacama Altiplano of Northern Chile (precipitation < 200 mm/year) provides excellent archives (paleosoils, shorelines of former lakes, glacial features) for studying past environmental conditions since the last cold maximum (ca 20,000 yr B.P.). The Swiss - Chilean research project "Climate Change in the arid Andes of Northern Chile" focuses on indications of significant long-term changes (e.g. warmer and/or wetter phases) during the past 20,000 years, which can be found in such archives (Hastenrath and Kutzbach, 1985; Kessler, 1985, 1991; Grosjean *et al.*, 1991; Grosjean, 1992). In order to understand long-term environmental changes and their interrelationship with previous high lake levels in the Altiplano, studies of short- to medium-term fluctuations in the budget of open water bodies are fundamental. Remote sensing is an excellent tool to determine such fluctuations of the water surface of lakes and salars. These changes have to be interpreted as a response function to climatic impact, e.g., precipitation and evaporation.

The study area (Fig. 1.) is situated in the buffer zone between the tropical and ectropical precipitation belts (23°S - 24°S).

The extreme aridity of the region is due to the synergistic interaction between subsiding anticyclonic air masses, the drying effect of the cold Humboldt current, and the moisture-blocking mountain chain of the high Andes. Even in the Altiplano region at an

altitude of 4,000 m a.s.l., only 180 mm of precipitation per year are normal. Below 2,500 m a.s.l. hardly any rainfall can be registered. Therefore, the open water bodies on which this investigation focuses can only be found above 4,000 m a.s.l. in the Altiplano region. At this altitude, the strong evaporation rates of the Atacama desert are reduced to 2,300 mm per year, and the precipitation increases, as already mentioned. The water in these brines (normally called salars) is mostly very salty and shallow. In addition, some deep fresh water lakes also exist. For this study, eight catchments (Salars Aguas Calientes I, Tara, Pujsa, Tuyajto, Talar, Lakes Lejía, Miñiques and Miscanti, see Fig. 1), between 23°S and 24°S and with comparable altitude (3,950 - 4,300 m a.s.l.) were selected.

The period of extreme "(post)-El Niño-precipitation" in the North Chilean Altiplano between December 1983 and August 1984 has been chosen as a case study. For this period, the synoptic situation (Fuenzalida and Rutllant, 1986) and origin of precipitation based on isotope analysis (Aravena *et al.*, 1989) are well described for the adjacent area in the North.

## Database

This case study is based on four LANDSAT-MSS images (Frame Nr. 233/076) of November 28, 1983, January 15, 1984, March 19, 1984 and August 26, 1984. The MSS system contains four bands, covering the spectral range from 0.5µm - 0.6µm (band 1), 0.6µm -

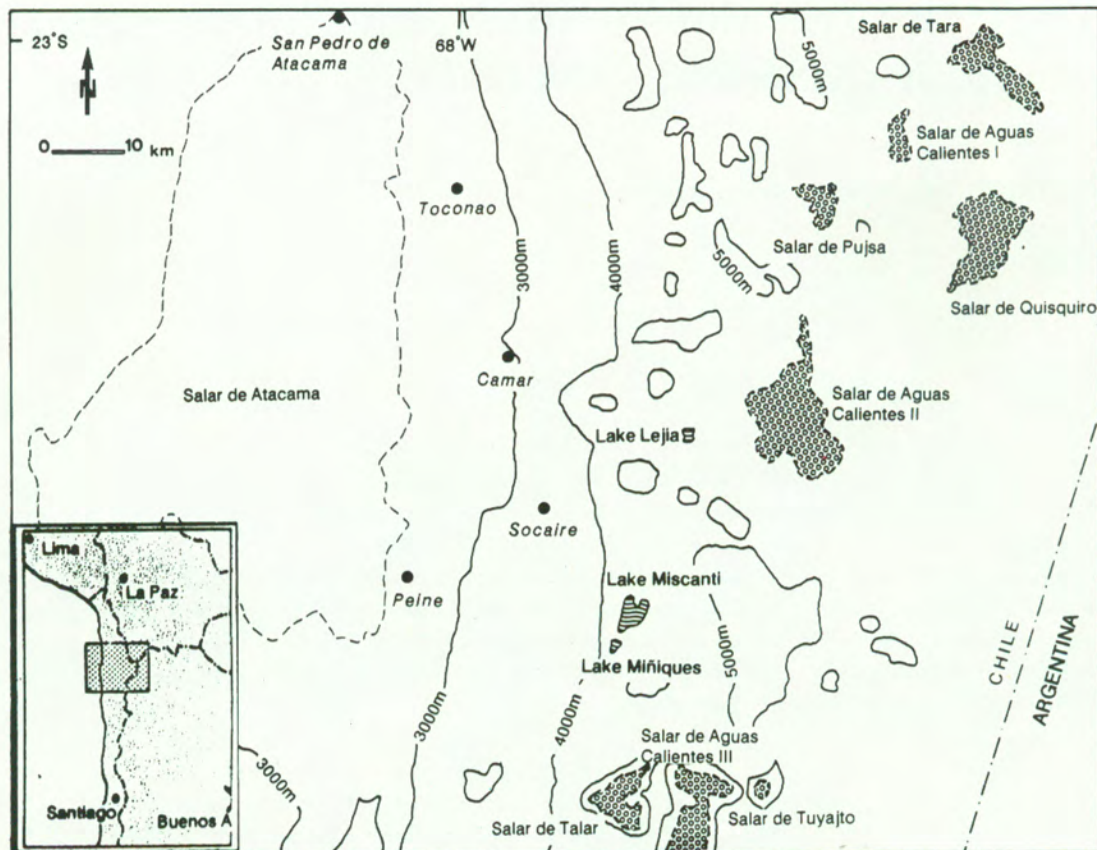


Figure 1 Map showing the research area.

0.7 $\mu\text{m}$  (band 2), 0.7 $\mu\text{m}$  - 0.8 $\mu\text{m}$  (band 3) and 0.8 $\mu\text{m}$  - 1.1 $\mu\text{m}$  (band 4). The pixel resolution of the geometrically corrected and resampled MSS data is 80m \* 80m. Figure 2 shows a subszene of such a Landsat-MSS full frame after geocorrection, of January 15, 1984, including the salars Tara, Aguas Calientes I and Pujsa.

Additionally, Landsat-TM data (quarter scene 4) of the same area, of March 28, 1990, was used. The TM system has an advanced spectral and geometric resolution compared with the MSS system (7 spectral bands: 0.45 $\mu\text{m}$  - 0.52  $\mu\text{m}$  (band 1), 0.52  $\mu\text{m}$  - 0.60  $\mu\text{m}$  (band 2), 0.63  $\mu\text{m}$  - 0.69  $\mu\text{m}$  (band 3), 0.76  $\mu\text{m}$  - 0.90  $\mu\text{m}$  (band 4), 1.55  $\mu\text{m}$  - 1.75  $\mu\text{m}$  (band 5), 10.4  $\mu\text{m}$  - 12.5  $\mu\text{m}$  (band 6), 2.08  $\mu\text{m}$  - 2.35  $\mu\text{m}$  (band 7) and a pixel resolution of 30 m \* 30 m).

On the same date as the satellite recording (March 28, 1990), field analysis of hydrologic parameters was carried out. Various lakes and salars were crossed by boat in order to measure the water depth and the salinity (electric conductivity) of the water. Twenty-nine samples of both parameters were taken. The sample sites were exactly positioned with the help of land surveys for a later identification of the coordinates of the sample sites.

Moreover, daily precipitation and monthly evaporation data from 12 ground stations were used to analyse the climatic situation during the time period of this case study. To extrapolate this climatic data into the study area, water catchment parameters (basin area, mean elevation of basin and elevation of water level (m a.s.l.)) were taken from topographic maps at a scale of 1:50.000.

## Methods

The idea of this study was to analyse all images (MSS and TM) in terms of changing water surface, water volume and salt content of the water, and to compare the results with extrapolated precipitation and evaporation data.

In order to detect the correct water surfaces of the lakes and salars and identify the sample sites in the TM satellite image, all images had to be geometrically corrected. This was done by using a linear transformation and a nearest-neighbour resampling in order to keep the original pixel values for further analysis. The transformation was applied to a Universal Transverse Mercator (UTM) map projection.

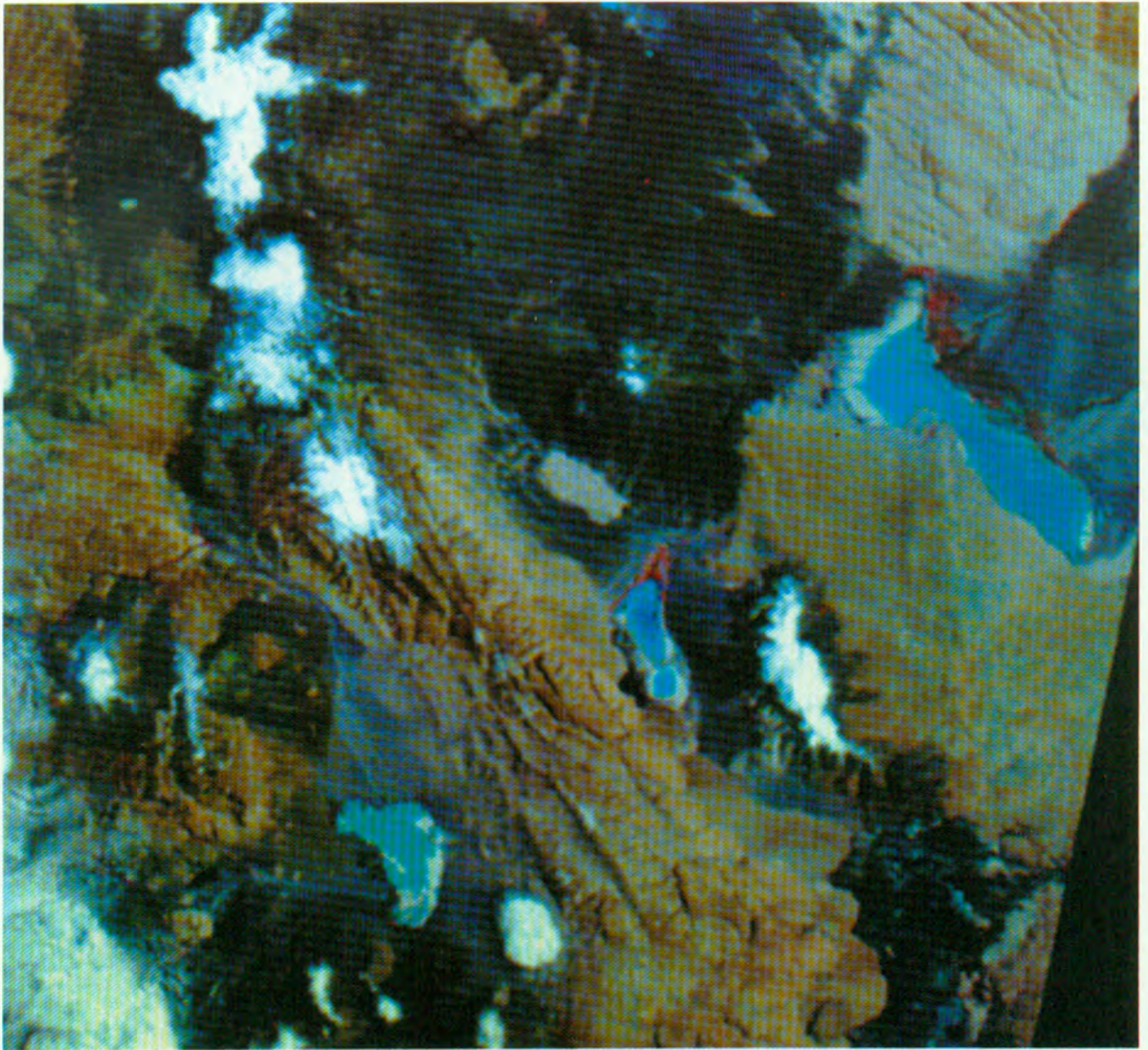


**Figure 2** Part of the geometrically corrected Landsat-MSS image of January 15, 1984, bands 4, 2 and 1 (in r, g, b), showing the salars Tara, Aguas Calientes I and Pujsa (from NE to SW).

### Water area delineation

The area of all lakes and salars was determined in every image. By doing so, a possible change in area due to precipitation or evaporation could easily be monitored.

As water is practically non-reflecting in the near-infrared range of the electromagnetic spectrum, it can easily be separated from other objects in the satellite image by using a simple density slicing technique (Work, 1976; Rose and Rosendahl, 1983). Figure 3 shows how this technique for deriving the water area of the Salar de Tuyajto in the TM data is used. The digital values belonging to the left peak in the histogram (in Fig. 3 the values  $\leq 22$ ) were classified as water, the values belonging to the right peak were classified as land (values  $> 22$  in Fig. 3). For determination of the water surface, MSS band 4 ( $0.8 \mu - 1.1 \mu$ ) and TM band

5 ( $1.55 \mu - 1.75 \mu$ ) were used.

It can easily be shown that this technique, although it is very simple, distinguishes clearly between land and water and determines the correct water surface. Figure 4 shows lakes Miscanti and Miniques in a three-dimensional diagram. The values of the z-axis correspond to the digital numbers of Landsat-TM band 5. Due to the very low values in this spectral range, the water surface becomes visible and easily distinguishable from the surrounding areas.

Unfortunately, the salars and lakes were sometimes covered by clouds or frozen, so that some results are missing (Figure 7 and Table 2).

### Salinity and water depth determination

Various authors have shown possible ways to compute water depth and water salinity in satellite

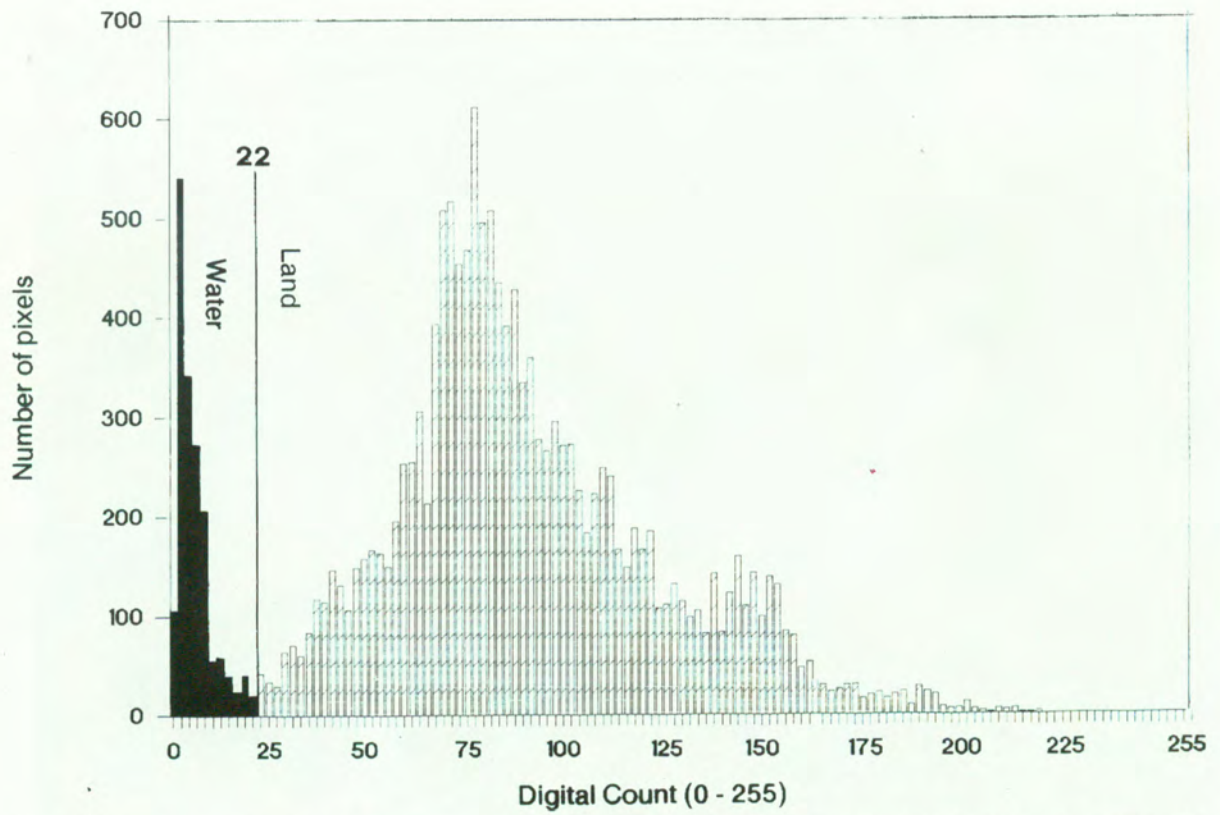


Figure 3 Density slicing technique to determine the water surface of Salar de Tuyajto, March 28, 1990. (Landsat-TM band 5:  $1.55 \mu - 1.75 \mu$ ).

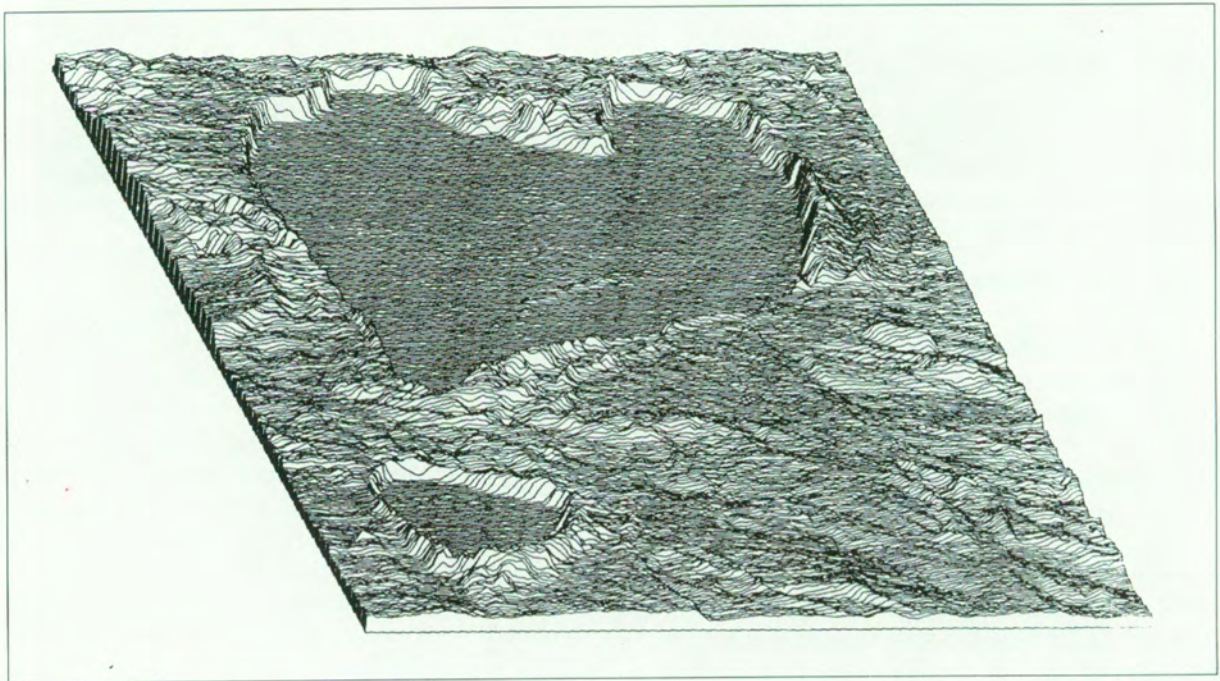


Figure 4 Lakes Miscanti and Miñiques shown as a three-dimensional diagram of Landsat-TM band 5 (z-axis = digital number).

data (Khorram, 1982, 1985; Khorram and Cheshire, 1985; Lathrop and Lillesand, 1986). Usually, empirical interrelationships between water parameters and digital satellite data are derived, using correlation and regression analysis. As only the TM image was calibrated by measuring the water parameters in the field, the resulting models had to be applied to the Landsat-MSS data as well.

Three different lakes and salars (Lake Lejla, Salar Tuyajto and Lake Miñiques) were crossed by boat on the date of the satellite overpass (March, 28, 1990). At twenty-nine sample sites water depth and water salinity were measured using a simple sounding lead and an electric conductivity measuring instrument (WTW-LF91). All sample sites were exactly positioned with help of land surveys. To compare the digital numbers in the TM data with the field measurements, the pixels corresponding to the coordinates of the sample sites had to be identified in the satellite image. This was possible after the geometric correction of the satellite image onto a Universal Transverse Mercator (UTM) map basis. The value of the pixel identified as corresponding to the sample site was replaced by the arithmetic mean of this pixel and its eight surrounding neighbours (Lillesand *et al.*, 1983; Ritchie, 1987). By creating such blocks of 3 \* 3 pixels, a less precise sample site identification is still acceptable. The mean values obtained were plotted against measured water depth and water salinity in all seven channels. The plots showed a logarithmic correlation between digital values and measured water salinity and a reciprocal correlation between digital values and water depth respectively. Therefore the logarithmic (water salinity computation) and the reciprocal (water depth computation) values of all channels were used as independent variables in the regression computations as well.

The stepwise multiple regression analysis was carried out separately for water depth and for water salinity. The F-values (significant at the 0.05 level of significance) were computed for all parameters and

used as decision-criteria. In each step the variable with the highest F-value was entered to the regression model. As no more variables reached the critical value (F = 3.0), the computation was stopped. The results of these computations are shown in Table 1.

Even though the results are empirical, they are statistically highly significant and very reliable. The only limitation that occurred is shown in Figure 5.

The water depth model is only reliable between 0 cm and 100 cm. Depths exceeding 100 cm no longer correlate with the digital satellite data. This limitation might be due to suspended sediments which reduced the penetration depth. The water salinity model could be used without any limitation. Results of these models, applied on various lakes and salars, are shown in Figures 8 and 9.

Furthermore, the water depth and the salinity should be computed for the four MSS scenes for studying possible changes during time. Application of the models derived from TM data to the MSS data is only possible if similar spectral bands are available on both TM and MSS. In the regression model for the parameter "water depth", TM band 2 (0.52 μ - 0.60 μ) could be replaced by MSS band 1 (0.5 μ - 0.6 μ) which covers practically the same spectral range (Williams *et al.*, 1984; Ritchie *et al.*, 1990). To transfer the electric conductivity model to the MSS data was of course not possible because the TM bands used (1, 4, 7, see table 1) do not exist on Landsat-MSS.

The digital numbers of the 8 bit-TM data and the 6 bit-MSS data are not directly comparable. Therefore, the digital data of all scenes were converted into physical units (radiance) using calibration tables (EOSAT, 1986) and satellite header information. The equation used are:

$$y = 0.4 + 0.186 * X_1$$

$$y = 0.3 + 0.209 * X_2$$

$$y = -0.28 + 0.117 * X_3$$

where y: radiance (mW\*cm<sup>-2</sup>\*sr<sup>-1</sup>)

x1: Digital number MSS band 1, until 5.

**Table 1** Regression models to compute electric conductivity (salinity) and depth of salar and lake water in the Northchilean Altiplano. Models are derived from Landsat-TM data.

Parameter	Equation	Variables	R - square
conductivity	$y = -49.03 + 16.42 * \ln(x_1) + 1.24 * x_4 - 2.06 * x_7$	y : conductivity (mS/cm) x <sub>1</sub> : digital count band 1 x <sub>4</sub> : digital count band 4 x <sub>7</sub> : digital count band 7	0.9657
water depth	$y = -25.6 + 5702.5 * (x_2)^{-1}$	y : water depth (cm) x <sub>2</sub> : digital count band 2	0.8280

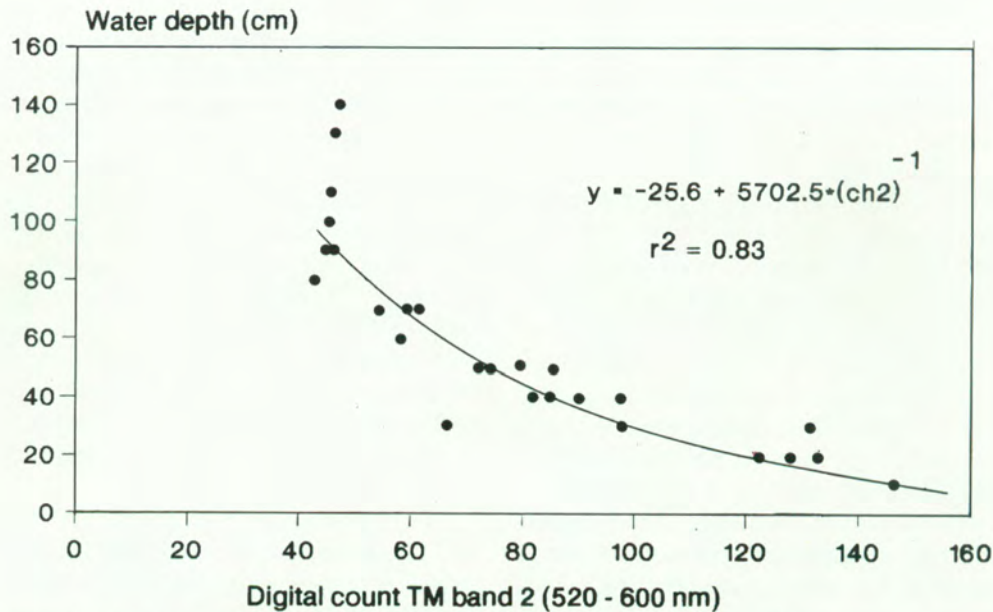


Figure 5 Water depth model using Landsat-TM band 2. The points represent surface measurements and corresponding digital values.

- April 1984
- x2: Digital number MSS band 1, since 6.
- April 1984
- x3: Digital number TM band 2

Another problem to be considered, was the different recording dates. The models derived from the TM data are only valid for March 28, 1990. The MSS images from 1983/84 were received under different illumination and atmospheric conditions. So, the MSS images had to be normalised before applying the TM model. These differences in sun elevation and atmospheric conditions for each image were corrected by adapting (stretching) the MSS band 1 histograms to the histogram of TM band 2. This method assumes that identical regions have nearly identical histograms if sun elevation and atmospheric conditions are the same, and clouds and snow cover are left apart. Figure 6 shows the different steps from MSS band 1 raw data (a) via the converted MSS data (b) to the adapted MSS data (c), which has a nearly equal histogram as TM band 2 (d). All four MSS scenes were processed in the same way; as shown for March 19, 1984 in Figure 6. Finally, this method allowed the application of the TM - water depth model to the MSS data.

## Results

The varying water areas of lakes and salars as detected in Landsat/MSS data were finally compared with climatic data. As the study area is a climatic no-man's land, no meteorological data from within the study area were available. Therefore, precipitation

and evaporation data registered at 12 stations bordering the study area were analysed and extrapolated to the different catchments. Precipitation data was grouped into 6 main precipitation events. The amount of precipitation in the salar catchments was then calculated for each event using a single linear regression depending on elevation. The same procedure was used to compute the evaporation amount during the study period. In some basins, the estimated amount of rainfall exceeded 180 mm in January 1984, which is higher than the annual mean. The time between February and August 1984 was less humid but wetter than normal overall. The results of the climatic analysis coincide with earlier investigations of these heavy rainfalls, which confirms the period between December 1983 to August 1984 as one of the most humid periods during the last decades (Fuenzalida and Rutllant, 1986). The response of the water bodies to these heavy rainfalls is shown in Fig. 7. In terms of "water surface" and "water volume", the different reaction of lakes and salars is significant. Lake level changes in the range of 30 cm do not result in a growing water surface due to steep shorelines. Small variations up to 0.1 km<sup>2</sup>, as recorded at Lake Lejía (Table 2), might be due to incorrect classification of mixed pixels. On the other hand, the salars show an extremely flat basin topography and rather impermeable ground characteristics. Therefore, the reaction of the shallow water bodies to any precipitation impact is very quick and significant (Fig. 7). The different behaviour of the catchments to the north (Tara, Pujsa, Aguas Callientes 1) and to the south (Tuyajto, Talar) of the study region

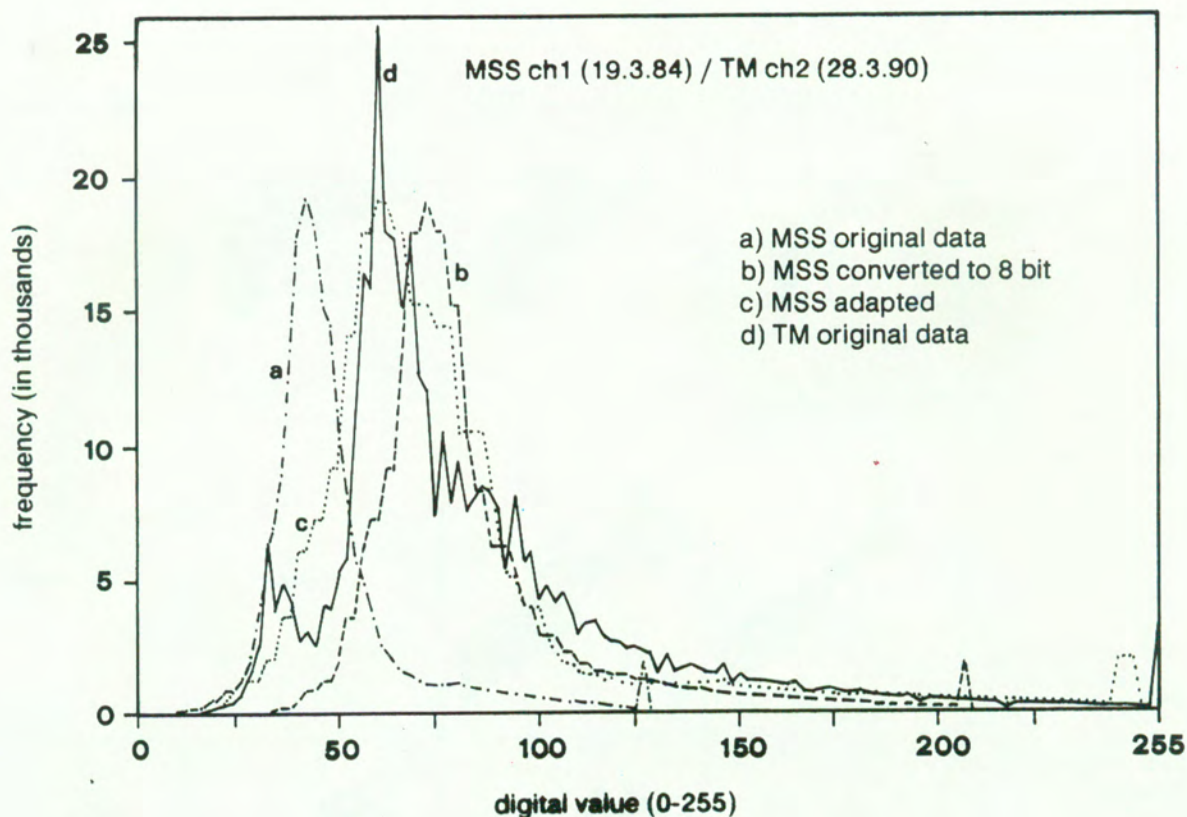


Figure 6 Histogram transformation for March 19, 1984.

is surprising and in terms of the time- and space-related pattern of the synoptic situation very important. For January 1984, the humid air masses of tropical and continental origin (Fuenzalida and Rutllant, 1986; Aravena *et al.*, 1989) might not have reached the southern part of the Altiplano at 24°S. Only the northern salars (Tara, Aguas Calientes I and Pujasa)

show a significant growth in water surface, due to the heavy rainfalls. Unfortunately, no data were available in January for the southern salars, Tuyajto and Talar. But obviously they did not react very clearly, as their water surfaces were practically as small in March 1984 as in November 1983. On the other hand, the southern salars grew between June and August while the Salar

Table 2 Changing water areas (km<sup>2</sup>) and water volumes (10<sup>6</sup>m<sup>3</sup>) of the lakes and salars as detected by Landsat-MSS.

Lake / Salar		28.Nov.1983	15.Jan.1984	19.Mar.1984	26.Aug.1984
Lake Lejia	area (m <sup>2</sup> )	1.98	2.04	2.08	-
	vol. (10 <sup>6</sup> m <sup>3</sup> )	1.875	2.036	2.044	-
Lakes Miscanti/Miñiques	area	-	14.18	14.13	14.10
	volume	-	-	-	-
Salar de Tara	area	17.31	26.44	-	-
	volume	10.330	15.159	-	-
Salar de Ag. Calientes	area	3.05	5.82	6.48	6.70
	volume	1.892	2.954	3.155	3.030
Salar de Pujasa	area	5.45	8.19	9.05	-
	volume	2.509	3.514	4.600	-
Salar de Tuyajto	area	2.31	-	2.23	2.46
	volume	0.450	-	0.469	0.474
Salar de Talar	area	0.07	-	0.28	6.15
	volume	0.065	-	0.287	1.971

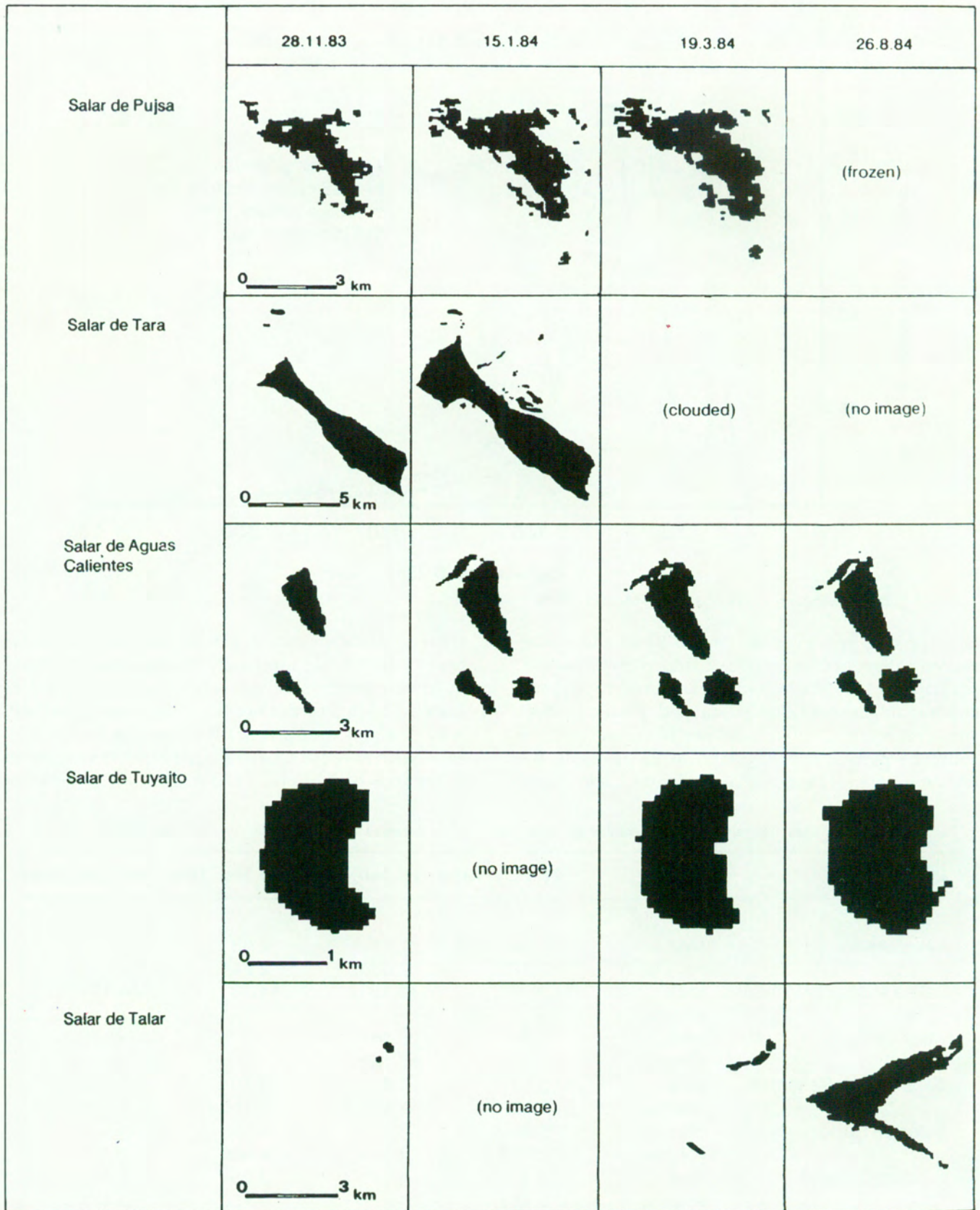


Figure 7 Dynamics of open water bodies from December 1983 to August 1984, as derived from Landsat-MSS.



de Aguas Calientes I in the north remained much the same. Although the humidity (June 1984) originated in the tropical part of the continent (Fuenzalida and Rutllant, 1986; Aravena *et al.*, 1989), precipitation linked with advection of cold air masses at higher altitudes was more abundant in the southern part of our research area. Data for August are lacking in the Tara and Puja catchments. At the same time the MSS image for August 1984 shows the southern part of the study area covered by snow, the probable reason for the growth of the water surface in the Tuyajto and Talar catchments (see Figure 7.).

Water depth and water salinity of lakes and salars were determined using the corresponding models, which were derived by comparing field measurements and digital satellite data.

Concerning salinity, a clear difference between the fresh water lakes and the brines in the salars occurred. The fresh water of lakes Miscanti and Miñiques hardly exceeds 15 mS/cm, whereas the saline brine water of the salars comes up to 100 mS/cm and more, which is extremely salty. Control measurements in different lakes and salars during field work showed that the results are very reliable and that the calculations lie in a range of  $\pm 5$  mS/cm, which is absolutely satisfactory. Two examples of these computations are shown in Figure 8 and 9.

As already shown in Figure 5, the water depth model is only reliable between 0 cm and 100 cm. Therefore, water depth could only be determined in the salars and Lake Lejia, as the depth of lakes Miscanti and Miñiques exceeded the reliable range of the model. Nevertheless, the model was very useful as the depth of the very shallow salars and Lake Lejia could be detected without any problems.

The water depth model was also applied to the MSS scenes, after substituting MSS band 1 for TM band 2, converting the digital numbers into radiances and normalising the different recording dates. By multiplying the pixel depths by the water surface, estimates of the changing water volumes in the salars during the time from November 1983 until August 1984 could be determined (see Table 2). These results show that not only the area of the salars but also their

water volume increased significantly during this humid phase.

## Conclusions

As this study shows, water depth and water salinity can be computed from satellite data using regression models, which are derived by comparing field measurements and digital satellite data. Furthermore, a model could be transferred from one satellite system to another (from TM to MSS) because of similar spectral bands on both systems: the digital numbers could be converted into physical units (radiances) and the scenes of different recording dates were normalised. Such applications of satellite data might be useful in future remote sensing studies because this procedure allows the application of various models derived from different satellite systems.

The areal and temporal distribution of precipitation in the arid North Chilean Altiplano has so far been an unsolved problem because of the lack of climatic stations. This study shows the possibility to use satellite data for this purpose by monitoring the areal variations of shallow salars and lakes. Their growing water bodies can easily be interpreted as the result of the spatial pattern of summer and winter precipitation. Nevertheless further investigations are needed to improve knowledge of the climate and hydrologic processes in this arid environment.

## Acknowledgements

This study is part of the project "Climate Change in the arid Andes" which is financed by the Swiss National Science Foundation (NF 21-27 824.89). We would like to thank B. Messerli and M. Grosjean, Institute of Geography, University of Berne, Switzerland, for their help before, during and after the field work. The Centro de Estudios Espaciales, Santiago, Chile and the Direccion Regional de Aguas, Antofagasta, Chile, made Landsat-MSS scenes and climatic data available. Finally this study was only possible due to the support of our Chilean friends Hugo Romero A. and A. Rivera (Universidad de Chile, Santiago).

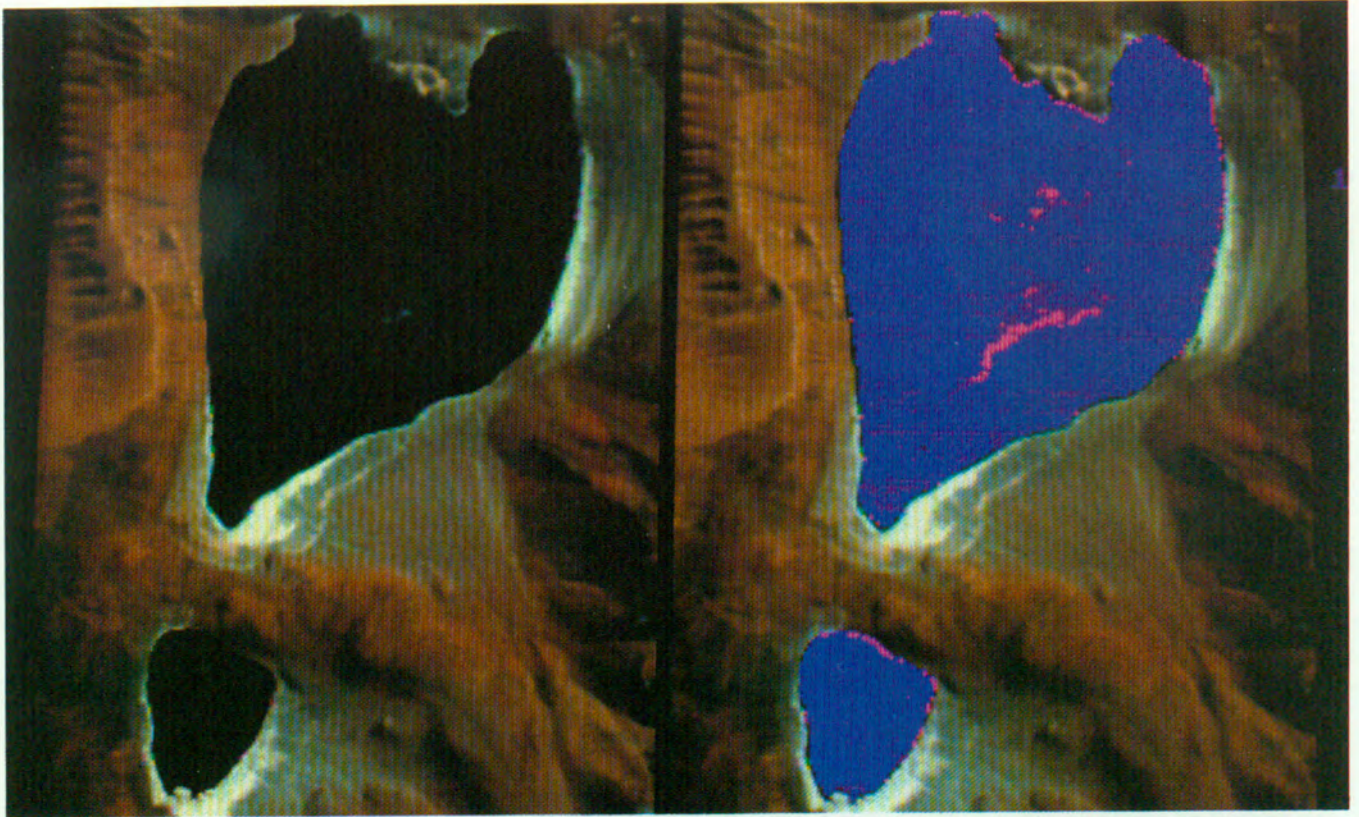


Figure 8 Computed salinity (mS/cm) of fresh water in lakes Miscanti and Miniques as derived from Landsat-TM data. On the left, colour composite using bands 4, 2 and 1 (r, g, b).

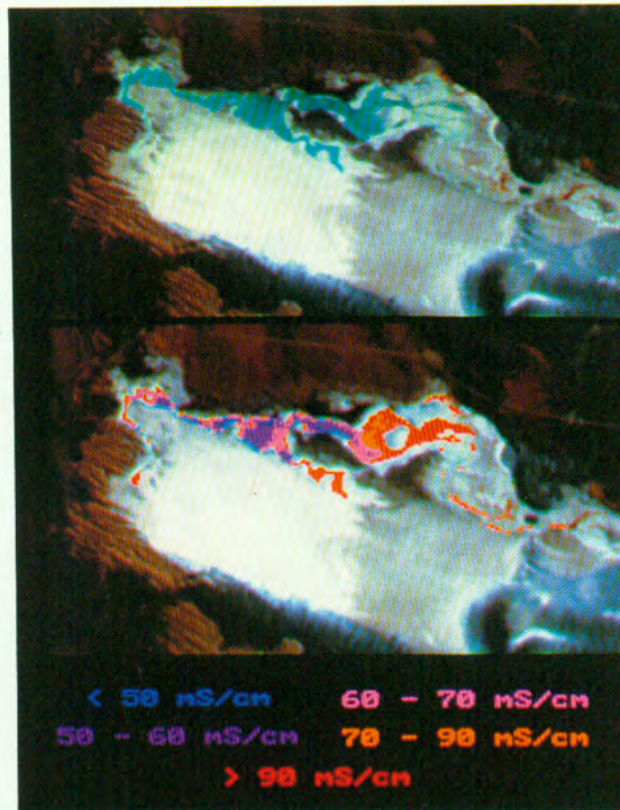


Figure 9 Computed salinity (mS/cm) of salar brine as derived from Landsat-TM data. Above, color composite of bands 4, 2 and 1 (r, g, b).

## References

- Aravena, R., Pena, H., Grilli, A., Suzuki, O. and Mordeckai, M., 1989: Evolucion isotopica de las lluvias y origen de las masas de aire en el Altiplano chileno. *IAEA-TECDOC-502: Isotope Hydrology Investigations in Latin America*, 129-142.
- Bartolucci, L.A., Robinson, B.A., Silva, L.F., 1977: Field measurements of the spectral response of natural waters. *Photogrammetric Engineering and Remote Sensing*, Vol. 43, No. 5, 595-598.
- EOSAT, 1986: Landsat Technical Notes No. 1.
- Fuenzalida, H. and Rutllant, J., 1986: Estudio sobre el origen del vapor de agua que precipita en el invierno altiplanico. Informe final, Universidad de Chile, 51 p.
- Grosjean, M., Messerli, B. and Schreier H., 1991: Seenhochstände, Bodenbildung und Vergletscherung im Altiplano Nordchiles: Ein interdisziplinärer Forschungsbeitrag zur Klimageschichte der Atacama. Erste Resultate. *Bamberger Geographische Schriften*, Bd. 11, 105-117.
- Grosjean, M., 1992: Zur Klimatologie und Paläoökologie des nordchilenischen Altiplano seit dem letzten Kaltzeitmaximum. Dissertation, University of Berne. 111p.
- Hastenrath, S., Kutzbach, J., 1985: Late Pleistocene climate and water budget of the South American Altiplano. *Quaternary Research* 24, 249-256.
- Kessler, A., 1985: Zur Rekonstruktion von spätglazialem Klima und Wasserhaushalt auf dem peruanisch - bolivianischen Altiplano. *Zeitschrift für Gletscherkunde und Glazialgeologie*, Bd. 21, 107-114.
- Kessler, A., 1991: Zur Klimaentwicklung auf dem Altiplano seit dem letzten Pluvial. *Freiburger Geographische Hefte* 32, 141-148.
- Khorram, S., 1982: Remote sensing of salinity in the San Francisco bay delta. *Remote Sensing of Environment*, 12, 15-22.
- Khorram, S., 1985: Development of water quality models, applicable throughout the entire San Francisco bay and delta. *Photogrammetric Engineering and Remote Sensing*, Vol. 51, No. 1, 53-62.
- Khorram, S. and Cheshire, H.M., 1985 Remote sensing of water quality in the Neuse river, North Carolina. *Photogrammetric Engineering and Remote Sensing*, Vol. 51 No. 3, 329-341.
- Lathrop, R.G. and Lillesand, T.M., 1986: Use of Thematic Mapper data to assess water quality in Green Bay and Central Lake, Michigan. *Photogrammetric Engineering and Remote Sensing*, Vol. 52, No. 5, 671-680.
- Lillesand, T.M. Johnson, W.L., Deuell, R.L., Lindstrom, O.M., Meisner, D.E., 1983: Use of landsat data to predict the trophic state of Minnesota lakes. *Photogrammetric Engineering and Remote Sensing*, Vol. 49, No. 2, 219-229.
- Ritchie, J.C., 1987: Comparison of Landsat MSS pixel array sizes for estimating water quality. *Photogrammetric Engineering and Remote Sensing*, Vol. 53, No. 11, 1549-1553.
- Ritchie, J.C., Cooper, C.M., Schiebe, F.R., 1990: The relationship of MSS and TM digital data with suspended sediments, chlorophyll and temperature in Moon Lake, Mississippi. *Remote Sensing of Environment*, Vol. 33, p. 137-148.
- Rose, P.W. and Rosendahl, P.C., 1983: Classification of Landsat data for hydrologic application, Everglades national park. *Photogrammetric Engineering and Remote Sensing*, Vol. 49, No. 4, 505-511.
- Williams, D.L., Irons, J.R., Markham, B.L., Nelson, R.F., Toll, D.L., Latty, R.S., Stauffer, M.L., 1984: A statistical evaluation of the advantages of Landsat Thematic Mapper data in comparison to Multispectral Scanner data. *IEEE transactions on geoscience and remote sensing*, Vol. 6E-22, No. 3, 294-302.
- Work, E.A., 1976: Utilization of satellite data for inventoring prairie lakes and ponds. *Photogrammetric Engineering and Remote Sensing*. Vol. 42, No. 5, 685-694.